Sample thickness and quantitative concentration measurements in Br *K*-edge XANES spectroscopy of organic materials

Alessandra C. Leri[a]* and Bruce Ravel[b]*

[a]Department of Natural Sciences, Marymount Manhattan College, 221 E 71st Street, New York, NY 10021, USA, and [b]National Institute of Standards and Technology, 100 Bureau Drive, MS 8370, Gaithersburg, MD 20899, USA. *E-mail: aleri@mmm.edu, bravel@bnl.gov

While XANES spectroscopy is an established tool for quantitative information on chemical structure and speciation, elemental concentrations are generally quantified by other methods. The edge step in XANES spectra represents the absolute amount of the measured element in the sample, but matrix effects and sample thickness complicate the extraction of accurate concentrations from XANES measurements, particularly at hard X-ray energies where the X-ray beam penetrates deeply into the sample. The present study demonstrates a method of quantifying concentration with a detection limit approaching $1 \, mg \, kg^{-1}$ using information routinely collected in the course of a hard X-ray XANES experiment. The XANES normalization procedure unambiguously separates the signal of the absorber from any source of background. The effects of sample thickness on edge steps at the bromine *K*-edge were assessed and an empirical correction factor for use with samples of variable mass developed.

Keywords: XANES; concentration measurement; thickness effect; thickness correction; bromine.

1. Introduction

Quantification of elemental concentrations in heterogeneous samples can be achieved using a variety of element-specific techniques, each of which carries certain limitations. Atomic absorption spectroscopy (AAS) and inductively coupled plasma mass spectrometry (ICP-MS) require destruction/extraction of samples, which may result in partial recoveries and underestimation of total concentrations. X-ray-based methods are non-destructive but subject to errors from sample composition. Particle probe techniques such as proton-induced X-ray emission (PIXE) and energy-dispersive X-ray spectroscopy (EDX) are sensitive only to the exposed surface of the sample. X-ray fluorescence (XRF) is bulk-sensitive but also susceptible to matrix effects, an issue that has been thoroughly explored in the standardization of XRF (Franzini *et al.*, 1972; Rousseau, 2006) as well as PIXE (Richter & Wätjen, 1981; Van Oystaeyen & Demortier, 1983) and EDX (Nielson, 1977) as quantitative techniques.

With X-ray absorption near-edge structure (XANES) spectroscopy, the typical goal of an experimental campaign is to determine the oxidation state and coordination environment of the element under study. In a XANES spectrum, the size of the edge jump is related to the concentration of the absorber element and, like the size of a fluorescence line in XRF, can be used to quantify concentration. The use of the XANES edge step for this purpose is not fundamentally different from quantification *via* XRF; indeed, in this context, the XANES is simply a sequence of XRF measurements at multiple energies. Because a quantitative determination of the size of

the edge step is an irreducible data-processing step in any systematic XANES or extended X-ray absorption fine structure (EXAFS) study, concentration quantification using the edge step can be readily incorporated into any XANES or EXAFS experiment.

Previous work (Leri *et al.*, 2006) has shown that, with careful standardization and sample preparation designed to obviate matrix effects, the edge jump in Cl XANES spectra can be used to quantify absolute chlorine concentrations in natural organic matter samples. At the Cl *K*-edge, X-ray beam penetration depth into natural organic matter samples is of the order of 40 μm, more than an order of magnitude smaller than the sample thicknesses in that study. For elements with hard X-ray edge energies, the depth of penetration of the X-rays is much greater, often transmitting through the sample entirely. This transmission is an experimentally useful property, as the transmitted beam is used for energy calibration by measurement of a reference material placed behind the sample. Because of the transmission of the X-ray beam, sample thickness is an important variable to consider in using XANES spectra for quantitative elemental analysis in the hard X-ray region.

Sample thickness has been considered in the application of XRF to quantitative elemental analysis (Van Dyck & Van Grieken, 1980; de Boer, 1991; Giauque, 1994; Sitko, 2005, 2009; Szczerbowska-Boruchowska, 2012). In this study, we present an accurate and purely empirical method of determining absorber concentration while correcting for sample thickness. This approach requires scant knowledge of sample composition and does not use tables of X-ray absorption coefficients or other fundamental constants. We demon-

strate this using Br K-edge XANES spectra of samples in a soft organic matrix.

2. Materials and methods

2.1. Sample preparation

Standards were prepared by dissolving poly(acrylic acid, sodium salt) (PAA) in appropriate volumes of 5 mM aqueous KBr to reach final target Br concentrations. These solutions were dried in a 313 K oven, and the resulting solids were pulverized in a mortar and pestle before being made into pellets using a 13 mm die set and a hydraulic laboratory press at 15000 lbs. For the standard curve, all pellets had a mass of 335 ± 2 mg, resulting in a thickness of 1.94 ± 0.01 mm, as measured with electronic calipers. For analysis of the effects of sample thickness, pellet mass was varied. Since PAA is hygroscopic, all standards were kept in a vacuum desiccator until just prior to analysis at the beamline. Natural organic matter samples were compressed into pellets of variable mass without dilution.

2.2. Br K-edge XANES spectroscopy

Br K-edge XANES spectra were collected at beamline X23A2 of the National Synchrotron Light Source. This is an unfocused bend-magnet beamline using a Si(311) monochromator of fixed-exit Golovchenko–Cowan (Golovchenko *et al.*, 1981) design. The incident, transmitted and reference X-ray intensities were measured using Ar-filled ionization chambers. XANES scans were obtained in fluorescence mode using a four-element energy-discriminating silicon-drift detector. The effect of detector dead time was corrected using the algorithm of Woicik *et al.* (2010). The hutch slits were adjusted to make a beam spot size of 4.5 mm (H) × 0.5 mm (V), which was roughly centered on the 133 mm^2 cross-sectional area of each sample pellet.

2.3. Quantitative analysis of spectral data

Raw data were processed using the *ATHENA* (Ravel & Newville, 2005) program. The energy of each Br K-edge XANES scan was calibrated using bromophenol blue as a reference transmission standard, aligning the peak of its white line to 13473.4 eV. The edge step of each spectrum was taken as the difference at 13472.0 eV between a line regressed through the pre-edge (13412 eV to 13442 eV) region and a quadratic polynomial regressed through the post-edge (13552 eV to 13652 eV) region of the Br K-edge XANES spectra. This way of quantifying the edge step represents the main distinction from the use of XRF to quantify the absorber concentration. Because so many energy points are used, the XANES spectrum represents a vast over-sampling of the size of the absorber emission line. The use of the pre- and post-edge polynomials provides an unambiguous distinction between the emission signal and any other physical process contributing photons in the same energy range. This allows accurate and precise quantification even of low absorber concentrations.

We approximate uncertainty in the size of the edge step by randomizing the end points of the energy ranges used to regress the pre- and post-edge polynomials, then computing an ensemble of 20 edge step measurements. The errors in edge step shown in Figs. 1 and 2 and in Table 1 are the standard deviations of those randomized ensembles and represent uncertainty from the determination of the polynomials used to extract the edge step.
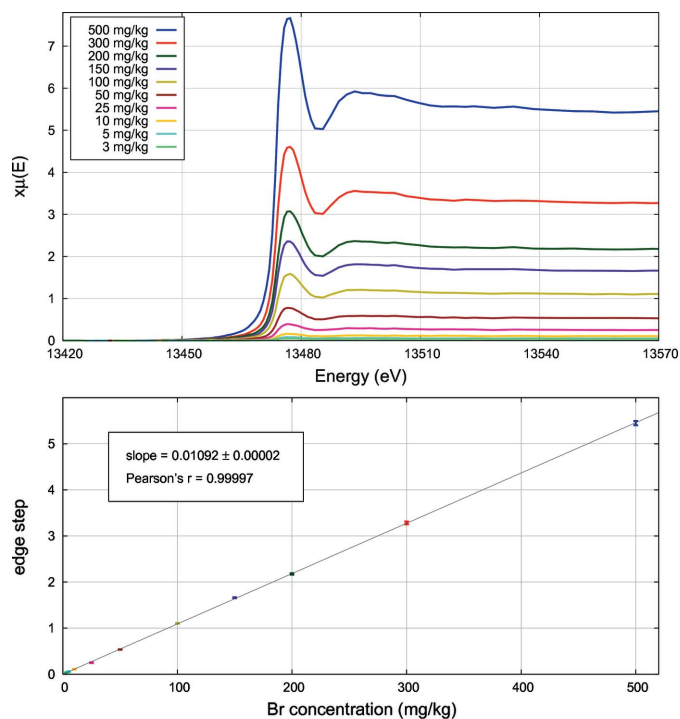
Figure 1
Relationship between the edge step of Br XANES spectra and Br concentration. These data were acquired for a series of KBr standards (335 mg pellets of 13 mm diameter) in a matrix of poly(acrylic acid, sodium salt).

3. Results and discussion

Representative Br K-edge XANES spectra for PAA-based standards of different Br concentration appear in Fig. 1. The pre-edge was subtracted from each spectrum, but the XANES spectra are shown unnormalized to highlight differences in edge step. For standard pellets, which are of constant mass and thickness, there is a linear relationship between the edge step of Br XANES spectra and the concentration of Br (Fig. 1, bottom). The edge step depends on the gains of the electronic signal processing and on the detector position relative to the sample, so it is essential to generate a standard curve relevant to the specific experimental conditions. Beamline X23A2 is equipped with a movable stage and sufficient range of motion in the vertical direction to allow analysis of several samples on the same mount. Once the initial Br calibration curve was established (Fig. 1, bottom), the detector was placed at the same position for each subsequent measurement to ensure that the measured edge step of a PAA-based quantitative KBr standard mounted alongside the other samples fell along the calibration line.

The PAA matrix chosen for the standards has similar interaction with the X-ray beam as natural organic matter samples (Leri *et al.*, 2006). Thus, we can use calibration curves like that in Fig. 1 to determine the total Br concentration in sample pellets. However, available quantities of sample material can fall below the target pellet mass of 335 mg. To develop a correction factor for underweight samples, we examined the relationship between edge step and sample thickness for Br standards at 300 mg kg^{-1} (Fig. 2) and 100 mg kg^{-1} (not shown). The results reveal a non-linear relationship between sample thickness or mass and the XANES edge step. This is attributable to attenuation of the incident beam as it enters the sample as well as the greater likelihood that fluorescence emitted from deeper within the sample will be reabsorbed by the sample matrix before

arriving at the detector. This effect is well known (Compton, 1929; Tröger *et al.*, 1992; Castañer & Prieto, 1997; Pfalzer *et al.*, 1999) to result in an energy-dependent attenuation of the EXAFS signal and has a functional form of $\{1 - \exp[-h(E)t]\}$ where t is the sample thickness and $h(E)$ depends on the absorption of the matrix at both the incident and fluorescence energies as well as on the angle of the sample surface relative to the incident beam. Calculation of $h(E)$ would require detailed knowledge of the sample composition, orientation and morphology. Instead, we account for the energy-dependent response of the sample using the post-edge quadratic polynomial and treat $h(E)$ as a constant to be determined empirically. The side panels of Fig. 2 show fits to the measured edge steps using equation (3) below.

Correction factors can be interpolated using either sample mass or thickness as the independent variable. Both are shown in Fig. 2. For the sample calculation below, we use the parameters extracted from the fit to the sample mass data. Approximating the dependence of edge step ($\hat{E}$) on sample mass by the expression for p shown below, we generate a correction factor c for any sample mass m_1, with reference to the mass of the calibration standards (m_0),

$$\hat{E}(m_0) = c(m_1)\,\hat{E}(m_1), \tag{1}$$

where

$$c(m_1) = p(m_0)/p(m_1) \tag{2}$$

and

$$p(m) = a_1\big[1 - \exp(-a_2 m)\big]. \tag{3}$$

This interpolation gives similar correction factors regardless of whether the terms a_1 and a_2 are determined from the mass data in Fig. 2 (300 mg kg^{-1}) or from the similar data measured on the 100 mg kg^{-1} samples. Taking $m_0 = 335$ mg, in accordance with the calibration curve in Fig. 1, and $m_0 = 300$ mg as a representative sample mass, then $c(300) = 1.032$ using the result shown in Fig. 2.

With the fits to the data shown in Fig. 2 using equation (3), we compute correction factors for sample pellets of different masses. To test this correction, we analyzed two natural organic matter samples of varying mass made from the same material (thus having the same
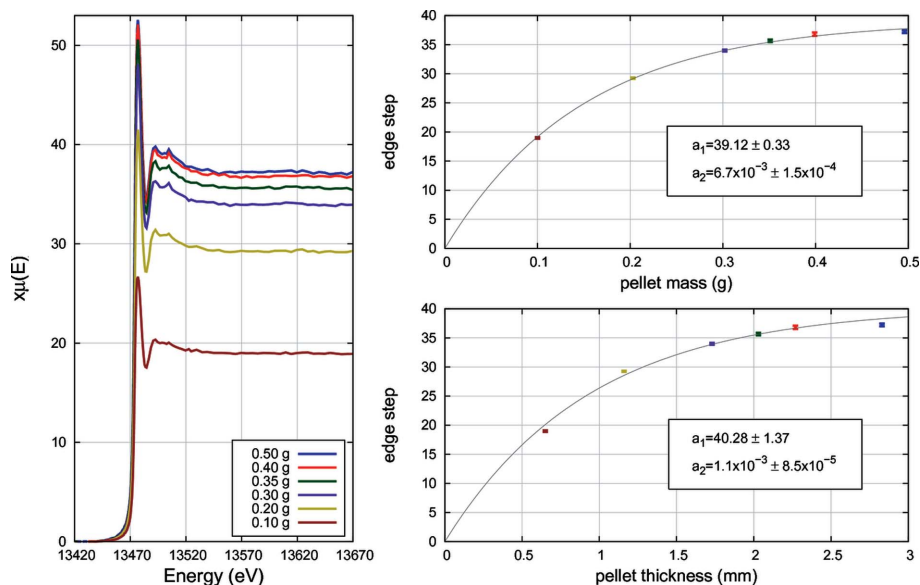
Table 1
Test of edge-step correction using natural organic matter samples of the same composition but different mass.

Uncertainties in measured edge step are explained in §2.3. The error in the corrected edge step is the result of propagating uncertainties in edge-step measurements, a_1 and a_2, through equations (1)–(3).

Parameter in equations (1) and (2)	Sample mass (mg)	Measured edge step	Correction factor $c(m_1)$	Corrected edge step $\hat{E}(m_0)$	Percent error
m_0	347	0.0805 ± 0.0040	1.805		
m_1	103	0.0461 ± 0.0023		0.0832 ± 0.0046	3.4%

Br content), then used equations (1)–(3) to correct the edge step of the lighter sample, $m_1 = 103$ mg, with reference to the heavier sample, $m_0 = 347$ mg. The results are shown in Table 1. The corrected edge step for the light sample is within measurement uncertainty and differs in value by only 3.4%.

To convert the measured edge steps for the samples in Table 1 into Br concentrations, we can correct each of them using equations (1)–(3) with $m_0 = 335$ mg, then determine concentration using the linear equation from the relevant calibration curve, in this case the inset of Fig. 1. This gives [Br] = 7.3 mg kg^{-1} for the 347 mg sample and [Br] = 7.6 mg kg^{-1} for the 103 mg sample. Calculating Br concentrations from the uncorrected edge steps would have given values of 7.4 and 4.2 mg kg^{-1}, respectively.

With this correction procedure, reliable bulk concentrations are determined in the course of a XANES experiment. Because this is a purely empirical approach to concentration measurement, it does require generation of calibration curves analogous to those in Figs. 1 and 2. It also requires that the matrix for the calibration standards closely resemble the absorption properties of the samples, just as with XRF measurements (Van Dyck & Van Grieken, 1980). In this case, PAA was chosen because its absorption properties are comparable with those of natural organic samples and because its solubility allows for production of homogeneous standards for the calibration data. More mineral-rich samples might require standards in an appropriate inorganic matrix.

Because it relies on the measured edge steps of an ensemble of experimental spectra, quantities that are required to interpret either XANES or EXAFS data, this procedure can be easily incorporated into any experimental campaign. Although a similar empirical formalism could be achieved by measuring the relevant emission peak at a single energy well above the absorption edge, there are certain advantages to the use of the XANES or EXAFS edge step, aside from the fact that edge-step values are already available as an irreducible step in the interpretation of the data ensemble. The determination of the polynomials using multiple energy points provides a way of distinguishing the emission signal from any source of background and of performing a defensible analysis of the uncertainty in the concentration measurement.

Figure 2
Relationship between the edge step of Br XANES spectra and thickness/mass of 300 mg kg^{-1} [Br] standard pellets. The fitted values of the parameters of equation (3) are shown as insets.

(Fig. 2 mass panel insets)
$a_1 = 39.12 \pm 0.33$
$a_2 = 6.7 \times 10^{-3} \pm 1.5 \times 10^{-4}$

(Fig. 2 thickness panel insets)
$a_1 = 40.28 \pm 1.37$
$a_2 = 1.1 \times 10^{-3} \pm 8.5 \times 10^{-5}$

(Spectra legend)
0.50 g
0.40 g
0.35 g
0.30 g
0.20 g
0.10 g

short communications

References

Boer, D. K. G. de (1991). *Spectrochim. Acta B*, **46**, 1433–1436.
Castañer, R. & Prieto, C. (1997). *J. Phys. III Fr.* **7**, 337–349.
Compton, A. H. (1929). *Philos. Mag.* **8**, 961–977.
Franzini, M., Leoni, L. & Saitta, M. (1972). *X-ray Spectrom.* **1**, 151–154.
Giauque, R. D. (1994). *X-ray Spectrom.* **23**, 160–168.
Golovchenko, J. A., Levesque, R. A. & Cowan, P. L. (1981). *Rev. Sci. Instrum.* **52**, 509–516.
Leri, A. C., Hay, M. B., Lanzirotti, A., Rao, W. & Myneni, S. C. B. (2006). *Anal. Chem.* **78**, 5711–5718.
Nielson, K. K. (1977). *Anal. Chem.* **49**, 641–648.
Pfalzer, P., Urbach, J. P., Klemm, M., Horn, S., denBoer, M. L., Frenkel, A. I. & Kirkland, J. P. (1999). *Phys. Rev. B*, **60**, 9335–9339.
Ravel, B. & Newville, M. (2005). *J. Synchrotron Rad.* **12**, 537–541.
Richter, F. W. & Wätjen, U. (1981). *Nucl. Instrum. Methods*, **181**, 189–194.
Rousseau, R. M. (2006). *Spectrochim. Acta B*, **61**, 759–777.
Sitko, R. (2005). *X-ray Spectrom.* **34**, 11–18.
Sitko, R. (2009). *Spectrochim. Acta B*, **64**, 1161–1172.
Szczerbowska-Boruchowska, M. (2012). *X-ray Spectrom.* **41**, 328–337.
Tröger, L., Arvanitis, D., Baberschke, K., Michaelis, H., Grimm, U. & Zschech, E. (1992). *Phys. Rev. B*, **46**, 3283–3289.
Van Dyck, P. M. & Van Grieken, R. E. (1980). *Anal. Chem.* **52**, 1859–1864.
Van Oystaeyen, B. & Demortier, G. (1983). *Nucl. Instrum. Methods Phys. Res.* **215**, 299–313.
Woicik, J. C., Ravel, B., Fischer, D. A. & Newburgh, W. J. (2010). *J. Synchrotron Rad.* **17**, 409–413.